Journal of Mathematical Research with Applications
Sept., 2022, Vol. 42, No. 5, pp. 523–538
DOI:10.3770/j.issn:2095-2651.2022.05.008
Http://jmre.dlut.edu.cn

Entropy Generation and Thermal Radiation Effects on Nanofluid over Permeable Stretching Sheet

S. K. ASHA*, G. MALI
Department of Mathematics, Karnatak University, Dharwad 580003*, India*

Abstract In the present paper, effects of entropy generation and nonlinear thermal radiation on Jeffery nanofluid over permeable stretching sheet with partial slip effect were analyzed. The suitable similarity transformation is utilized for the reduction of a set of governing equations, which are solved by using Differential Transformation Method (DTM) with the help of symbolic software MATHEMATICA. The accuracy of impact of slip parameter on coefficient of skin friction by using DTM and numerical method (Shooting technique with fourth-order Runge-Kutta) is illustrated and good agreement is found. Further, velocity, temperature, nanoparticle volume fraction and entropy generation profiles are shown graphically and studied in detail for various physical parameters. We notice that, as slip parameter rises the velocity and entropy generation profile rises. Enhancement in the effect of nonlinear thermal radiation reduces the entropy generation.

Keywords stretching sheet; partial slip; permeable; nonlinear thermal radiation; entropy generation; Jeffrery nanofluid

MR(2020) Subject Classification 76A05; 34A34; 35A24; 76D05

1. Introduction

In several industrial and engineering processes, prominent importance of flow over stretching sheet can be seen, for instance, in polymer sheets extrusion, production of glass–fiber and paper, wire drawing, metal–spinning. In these cases, the rate of cooling and stretching is very much needed in obtaining the desired final quality of the product. The theory of flow over a stretching plate was coined by Crane [1]. After this work, several researchers gave their attention towards the flow over stretching surface and a lot of work has been done on this problem [2–6]. In the above cited literature, fluid velocity is taken zero at the solid boundary. But in certain cases, replacement of no slip boundary condition by the partial slip boundary condition is more required. A slip boundary condition in which fluid velocity is directly proportional to tangential stress was initiated by Navier [7]. Further, Navier boundary conditions were extended by Shikhmurzaev [8], Choi et al. [9] and Matthews [10]. Consideration of heat generation/absorption and slip boundary conditions over stretching sheet was studied by Das et al. [11] and Dodda et al. [12]. Some works related to partial slip boundary conditions can be seen in [13–16]. A remarkable variation in the flow field through the bounding surface can be seen in the residence of suction or injection of a

Received January 28, 2022; Accepted May 21, 2022
* Corresponding author
E-mail address: ashask@kud.ac.in (S. K. ASHA); maligayitri@gmail.com (G. MALI)

fluid. In practice, suction tries to enhance the skin friction and opposite behaviour can be seen in injection. On suction or injection, a considerable investigation has been conducted by many researchers; few are given in the ref. [17–20].

Effect of radiation heat transfer has important applications in physics, various engineering branches, industries, material science such as in the design of equipments, glass generation, gas turbines, satelights, furnace design, propulsion system, power plants for inter planetary fights which operate at high temperatures. Hence, in such processes nonlinear thermal radiation effects cannot be neglected. Many researchers utilized radiation effect which was examined by linearized Rosseland approximation. But, this linearized Rosseland approximation is valid only for smaller variation of temperature in the middle of the plate and ambient fluid. But, non-linearized Rosseland approximation is sensible and plays an important role for larger variation of temperature. By using non-linearised Rosseland approximation one can solve the problems for both small and large variations of temperature on boundary and the ambient fluid. But, on boundary layer the impacts of thermal radiation are known very little. Hossain and Takhar [21], Takhar et al. [22] and Hossain et al. [23] studied in detail radiation impacts on heat transfer problems. In the temperature equation, addition of radiation effects gives highly nonlinear partial differential equation.

Nowadays, interest of many researchers is on entropy of thermodynamical systems. In heat transfer processes, the presence of entropy generation is customary and is related to thermodynamic irreversibility. Such irreversibility are viscous dissipation, mass diffusion, magnetic effect and heat transfer. The study of all these irreversibility helps us to recognize the irreversibility connected with many components and to ignore the loss of accessible energy. This instruction helps us to design thermal systems, guess the price of engineering systems and optimize complex systems. Entropy generation was initiated by Bejan [24]. Second law of thermodynamics is the reason why increment is possible in such irreversibility. Because of this increment in irreversibility, efficiency of various types of thermodynamical systems increases. Thus entropy generation plays a major part in finding out the demonstration of thermal machines such as heat engines, power plants, heat pumps and so on. Some more works on entropy generation can be seen in [25–29].

In real world, we can see many applications of non–Newtonian fluids in different fields such as food processing industries, chemical engineering, mechanical engineering and so on. Because of this reason, attention of several researchers is towards the study of transport phenomena of non-Newtonian fluids and Jeffrey model is one among them. This model describes the impact of relaxation and retardation times. It shows linear viscoelastic feature and has many applications in polymer sector. Jeffrey originated the retardation concept to study the wave propagation appearance in the earth's mantle and at the end in the description of the Jeffrey temperature flux model. Relaxation time explains the time taken by the fluid to bring back from the changed position to their original stability state. Some other woks on Jeffrey nanofluid can be seen in [30–36].

There are a number of analytical, semi-analytical and numerical methods used to solve non-

linear differential equations. DTM is famous among them. Because, DTM has some advantages over other methods. Perturbation techniques depend on small or large quantities but DTM is independent of them. Therefore, for nonlinear problems containing governing equations and boundary/initial conditions having small or large quantities or not, DTM can be applied. Unlike analytical methods, DTM does not need to compute auxiliary parameter, initial guesses and auxiliary linear operator and solves equations directly. DTM helps us to demonstrate the solutions of a given nonlinear problem by utilizing Padé approximant and Ms-DTM or other modifications.

The partial slip and nonlinear thermal radiation effects on Jeffrey nanofluid over permeable stretching sheet is not yet studied. Impacts of thermal radiation, on boundary layer are known very little in literature. Non-linearized Rosseland approximation is sensible and plays an important role for larger variation of temperature and one can solve the problems for both small and large variations of temperature on boundary and the ambient fluid. In most of the literature, entropy generation is studied by using stretching sheet with various nanofluids and effects. But, entropy generation by considering Jeffrey nanofluid model and permeable stretching sheet by using DTM is not yet studied. We get the ordinary differential equations by utilizing appropriate similarity transformation. We get highly nonlinear reduced ordinary differential equations which are solved by using semi-analytical method known as differential transformation method (DTM) [37–39]. We obtain an analytical solution in terms of polynomial by using this method. DTM is different from traditional higher–order Taylor series method. To calculate higher orders, Taylor series method becomes very expensive. Therefore, DTM is another tool to have analytic Taylor series solution of differential equations and can be applied directly to these nonlinear differential equations in the absence of discretization, linearization. Hence, the errors related to discretization cannot affect DTM. The accuracy of DTM and numerical method is illustrated and also matching between these two methods can be seen in figure. Similarly, for various differential equations the accuracy of solutions by using analytical, semi–analytical and numerical methods can be seen in [40–45]. Further, velocity, temperature, nanoparticle volume fraction and entropy generation profiles are displayed graphically and studied in detail for various physical parameters.

2. Mathematical formulation

As shown in Figure 1, a stretching flat sheet is moving along the horizontal direction with velocity $\overleftrightarrow{U_w} = a\,x$ where $a > 0$ and a is constant parameter. The surface is permeable and suction or blowing occurs at the surface in vertical direction. Velocity of the fluid out of boundary layer is zero. The governing equations are given below [12, 18–20]

$$\frac{\partial \overleftrightarrow{U}}{\partial x} + \frac{\partial \overleftrightarrow{V}}{\partial y} = 0, \tag{2.1}$$

$$\frac{1+\lambda}{\gamma}(\overleftrightarrow{U}\frac{\partial \overleftrightarrow{U}}{\partial x} + \overleftrightarrow{V}\frac{\partial \overleftrightarrow{U}}{\partial y})$$

$$= \frac{\partial^2 \overleftrightarrow{U}}{\partial y^2} + \lambda_1 (\overleftrightarrow{U} \frac{\partial^3 \overleftrightarrow{U}}{\partial x \partial y^2} + \overleftrightarrow{V} \frac{\partial^3 \overleftrightarrow{U}}{\partial y^3} - \frac{\partial \overleftrightarrow{U}}{\partial x} \frac{\partial^2 \overleftrightarrow{U}}{\partial y^2} + \frac{\partial \overleftrightarrow{U}}{\partial y} \frac{\partial^2 \overleftrightarrow{U}}{\partial x \partial y}), \tag{2.2}$$

$$\overleftrightarrow{U} \frac{\partial \overleftrightarrow{T}}{\partial x} + \overleftrightarrow{V} \frac{\partial \overleftrightarrow{T}}{\partial y} = \alpha \frac{\partial^2 \overleftrightarrow{T}}{\partial y^2} + \tau \big[D_B (\frac{\partial \overleftrightarrow{C}}{\partial y} \frac{\partial \overleftrightarrow{T}}{\partial y}) + \frac{D_T}{T_\infty} (\frac{\partial \overleftrightarrow{T}}{\partial y})^2 \big] - \frac{1}{(\rho c)_p} \frac{\partial q_r}{\partial y}, \tag{2.3}$$

$$\overleftrightarrow{U} \frac{\partial \overleftrightarrow{C}}{\partial x} + \overleftrightarrow{V} \frac{\partial \overleftrightarrow{C}}{\partial y} = D_B \frac{\partial^2 \overleftrightarrow{C}}{\partial y^2} + \frac{D_T}{T_\infty} \frac{\partial^2 \overleftrightarrow{T}}{\partial y^2}. \tag{2.4}$$

Where, $\overleftrightarrow{U}$ and $\overleftrightarrow{V}$ are velocity components along the x and y direction, respectively. μ is the coefficient of fluid viscosity, ρ_f is density of the fluid, ρ_p is density of the nanoparticle, $(\rho c)_f$ is heat capacity of the base fluid, $(\rho c)_p$ is heat capacity of the nanoparticle, $\tau = \frac{(\rho c)_p}{(\rho c)_f}$ is the ratio of effective heat capacity of the nanoparticle material to heat capacity of the fluid, q_r is radiative heat flux, $\overleftrightarrow{T}$ is fluid temperature, $\alpha = \frac{k}{(\rho c)_f}$ is the thermal diffusivity of the fluid, k is the thermal coductivity, $\overleftrightarrow{C}$ is nanoparticle volume fraction, $\overleftrightarrow{T_\infty}$ is temperature of the fluid far away from the stretching sheet, $D_{\overleftrightarrow{T}}$ is Brownian diffusion coefficient, D_B is thermophoresis diffusion coefficient.

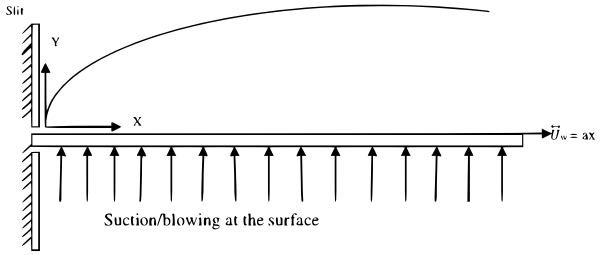

Figure 1 Schematic diagram of permeable stretching surface

By utilizing Rosseland approximation q_r,

$$q_r = \frac{-4\sigma^*}{3k^*} \frac{\partial \overleftrightarrow{T}^4}{\partial y} = \frac{-16\sigma^*}{3k^*} \overleftrightarrow{T}^3 \frac{\partial \overleftrightarrow{T}}{\partial y}, \tag{2.5}$$

the boundary conditions are as follows

$$\overleftrightarrow{U} = \overleftrightarrow{U_w} + L \frac{\partial \overleftrightarrow{U}}{\partial y}, \ \overleftrightarrow{V} = \overleftrightarrow{V_w}, \ \overleftrightarrow{C} = \overleftrightarrow{C_w}, \ \overleftrightarrow{T} = \overleftrightarrow{T_w} \text{ as } y = 0, \tag{2.6}$$

$$\overleftrightarrow{U} \to 0, \ \overleftrightarrow{T} \to \overleftrightarrow{T_\infty}, \ \overleftrightarrow{C} \to \overleftrightarrow{C_\infty} \text{ as } y \to \infty. \tag{2.7}$$

Non-dimensional similarity variables as follows

$$\eta = \frac{y}{x} (Re)^{\frac{1}{2}}, \ \psi = \overleftrightarrow{U_w} \, x (Re)^{\frac{-1}{2}} f(\eta), \ \theta(\eta) = \frac{\overleftrightarrow{T} - \overleftrightarrow{T_\infty}}{\overleftrightarrow{T_w} - \overleftrightarrow{T_\infty}}, \ \phi(\eta) = \frac{\overleftrightarrow{C} - \overleftrightarrow{C_\infty}}{\overleftrightarrow{C_w} - \overleftrightarrow{C_\infty}}, \tag{2.8}$$

where, η is similarity variable, ϕ is dimensionless nanoparticle volume fraction, f is dimensionless stream function, θ is dimensionless fluid temperature, ψ is stream function.

Where θ_w is temperature ratio parameter and is given below

$$\theta_w = \frac{\overleftrightarrow{T_w}}{\overleftrightarrow{T_\infty}}, \quad \theta_w > 1, \tag{2.9}$$

where $\psi(x, y)$ is defined as

$$\overleftrightarrow{U} = \frac{\partial \psi}{\partial y}, \quad \overleftrightarrow{V} = -\frac{\partial \psi}{\partial x}. \tag{2.10}$$

Eq. (2.1) is automatically satisfied by using (2.10) and Eqs. (2.2)–(2.4) are reduced into ordinary differential equations as given below

$$f''' + \beta\,(f''^2 - ff'''') + (1+\lambda)(ff'' - f'^2) = 0, \tag{2.11}$$

$$\begin{aligned}&(1+Rd)\theta'' + Pr(f\theta' + Nb\,\phi'\theta' + Nt(\theta'^2)) + \\ &Rd\big[(\theta_w - 1)^3\theta^3\theta'' + 3(\theta_w-1)^3\theta^2\theta'^2 + 3(\theta_w-1)\theta\theta''\big] + \\ &Rd\big[3(\theta_w-1)(\theta'^2) + 3(\theta_w-1)^2\theta^2\theta'' + 6(\theta_w-1)^2\theta\theta'^2\big] = 0,\end{aligned} \tag{2.12}$$

$$\phi'' + Le\,f\phi' + \frac{Nt}{Nb}\theta'' = 0. \tag{2.13}$$

Boundary conditions (2.6) and (2.7) are transformed as follows

$$f(0) = S,\ f'(0) = 1 + \delta\,f''(0),\ \theta(0) = 1,\ \phi(0) = 1 \text{ at } \eta = 0, \tag{2.14}$$

$$f' \to 0,\ \theta \to 0,\ \phi \to 0 \text{ as } \eta \to \infty. \tag{2.15}$$

The parameters are defined as

$$\begin{aligned}&Nb = \frac{(\rho c)_p D_B(\overleftrightarrow{C_w} - \overleftrightarrow{C_\infty})}{(\rho c)_f \gamma},\ Nt = \frac{(\rho c)_p D_{\overleftrightarrow{T}}(\overleftrightarrow{T_w} - \overleftrightarrow{T_\infty})}{(\rho c)_f \gamma\,\overleftrightarrow{T_\infty}},\ Pr = \frac{\gamma}{\alpha},\\ &Le = \frac{\gamma}{D_B}, Rd = \frac{16\sigma^*\overleftrightarrow{T_\infty}}{3kk^*},\ S = -\overleftrightarrow{V_w}(x)\sqrt{\frac{x}{\gamma\,\overleftrightarrow{U_w}}},\ Re = \frac{\overleftrightarrow{U_w}}{\gamma}\,x,\ \delta = L(\frac{a}{\gamma})^{\frac{1}{2}},\end{aligned} \tag{2.16}$$

where, Nb is Brownian motion parameter, Nt is thermophoresis parameter, Pr is Prandtl number, Rd is thermal radiation parameter, S is suction/injection parameter ($S > 0$ for suction and $S < 0$ for injection), Le is lewis number, Re is Reynolds number, δ is velocity slip parameter, $\overleftrightarrow{U_w}$ is velocity of the wall along the x axis, k^* is mean absorption coefficient, k is thermal conductivity, γ is kinematic viscosity, σ^* is Stefan-Boltzmann constant, $\overleftrightarrow{T_w}$ is temperature at the surface, $\overleftrightarrow{C_w}$ is nanoparticle volume fraction at wall temperature, $\overleftrightarrow{C_\infty}$ is ambient nanoparticle volume fraction, α is thermal diffusivity.

Where C_f and Sh_x are given below

$$C_f = \frac{\tau_w}{\rho_f \overleftrightarrow{U_w}^2},\ Sh_x = \frac{x\,q_m}{D_B(\overleftrightarrow{C_w} - \overleftrightarrow{C_\infty})}, \tag{2.17}$$

where τ_w and q_m are given below

$$\tau_w = \frac{\mu}{1+\lambda}\big[\frac{\partial \overleftrightarrow{U}}{\partial y} + \lambda_1(\overleftrightarrow{U}\frac{\partial^2 \overleftrightarrow{U}}{\partial x \partial y} + \overleftrightarrow{V}\frac{\partial^2 \overleftrightarrow{U}}{\partial y^2})\big]_{y=o},\ q_m = -D_B(\frac{\partial \overleftrightarrow{C}}{\partial y})_{y=0}. \tag{2.18}$$

Here, τ_w is wall shearing stress, q_w is surface heat flux, q_m is surface mass flux, λ is relaxation to retardation times, λ_1 is retardation time, β is Deborah number, μ is dynamic viscosity of the base fluid, C_f is skin-friction coefficient, Sh_x is sherwood number.

Using Eqs. (2.6), (2.7), (2.17) and (2.18) is reduced as

$$C_f(Re)^{\frac{1}{2}} = \frac{1}{1+\lambda}[f''(0) + \beta\, f'(0)f''(0) - f(0)f'''(0)],\ (Re)^{\frac{-1}{2}} Sh_x = -\phi'(0). \tag{2.19}$$

3. Entropy generation analysis

The volumetric entropy generation equation is represented as [24–26]

$$\begin{aligned} S_{gen} =& \Big[\frac{1}{\overleftrightarrow{T_\infty}}(k + \frac{16\sigma^* \overleftrightarrow{T}^3}{3k^*})(\frac{\partial \overleftrightarrow{T}}{\partial y})^2\Big] + \\ & \Big[\frac{Rd\ D_B}{\overleftrightarrow{C_\infty}}(\frac{\partial \overleftrightarrow{C}}{\partial y})^2 + \frac{Rd\ D_B}{\overleftrightarrow{T_\infty}}(\frac{\partial \overleftrightarrow{T}}{\partial y})(\frac{\partial \overleftrightarrow{C}}{\partial y})\Big]. \end{aligned} \tag{3.1}$$

The above equation contains two effects:

(a) First part represents heat transfer irreversibility;

(b) Second part represents diffusive irreversibility.

The characteristics entropy generation is given below

$$S_0 = \frac{k(\overleftrightarrow{T_w} - \overleftrightarrow{T_\infty})^2}{\overleftrightarrow{T_\infty}^2\ x^2}. \tag{3.2}$$

The entropy generation number is

$$N_S = \frac{S_{gen}}{S_0}. \tag{3.3}$$

By using Eqs. (3.1)–(3.3)and Eq. (2.8), the dimensionless form of entropy generation is,

$$N_S = Re[1 + Rd(1 + \theta(\theta_w - 1))^3](\theta')^2 + Re\ \varepsilon(\frac{\Omega}{\Sigma})^2(\phi')^2 + Re\ \varepsilon(\frac{\Omega}{\Sigma})\theta'\phi', \tag{3.4}$$

where

$$Re = \frac{\overleftrightarrow{U_w}(x)}{\gamma}x,\ \Delta T = (\overleftrightarrow{T_w} - \overleftrightarrow{T_\infty}),\ \Sigma = \frac{\overleftrightarrow{T_w} - \overleftrightarrow{T_\infty}}{\overleftrightarrow{T_\infty}},\ \Omega = \frac{\overleftrightarrow{C_w} - \overleftrightarrow{c_\infty}}{\overleftrightarrow{C_\infty}},\ \varepsilon = \frac{Rd\ D_B\ \overleftrightarrow{C_\infty}}{k}, \tag{3.5}$$

where, N_S is dimensionless entropy number, $\sum$ is dimensionless temperature difference, Ω, ε are dimensionless constant parameters, ΔT is temperature difference.

4. Method of solution

The differential transform of function $u(\eta)$ for j^{th} derivative is,

$$U[j] = \frac{1}{j!}[\frac{d^j u}{d\eta^j}]. \tag{4.1}$$

Here, $u(\eta)$ gives the main function and $u(j)$ is transformed function. Inverse differential transform is,

$$u(\eta) = \sum_{j=0}^{\infty} F(j)[(\eta - \eta_0)^j]. \tag{4.2}$$

In real world problems, we represent $u(\eta)$ in finite series and given as,

$$u(\eta) = \sum_{j=0}^{c} U(j)[(\eta - \eta_0)^j]. \tag{4.3}$$

Here, c is calculated by the convergence in this study. The reduced governing Eqs. (2.11)–(2.13) with Eqs. (2.14) and (2.15) and entropy generation Eq. (3.4) are resolved by utilizing DTM method and we get the following Eqs. (4.4)–(4.7)

$$\begin{aligned}
&(h+1)(h+2)(h+3)F(h+3)+\\
&\beta\Big[\sum_{b=0}^{h} F(-b+h)(-b+h+1)(-b+h+2)F(-b+h+2)\Big]-\\
&\beta\Big[\sum_{b=0}^{h} F(-b+h)(b+1)(b+2)(b+3)(b+4)F(b+4)\Big]+\\
&(1+\lambda)\Big[\sum_{b=0}^{h} F(-b+h)(b+1)(b+2)F(b+2)\Big]-\\
&(1+\lambda)\Big[\sum_{b=0}^{h} F(-b+h+1)(-b+h+1)(b+1)F(b+1)\Big] = 0,
\end{aligned} \tag{4.4}$$

$$\begin{aligned}
&(1+Rd)(h+1)(h+2)T(h+2) + Pr\Big[\sum_{b=0}^{h}(b+1)T(b+1)F(-b+h)\Big]+\\
&Pr\Big[Nb\sum_{b=0}^{h}(b+1)(-b+h+1)P(b+1)T(-b+h+1)\Big]+\\
&Pr\Big[Nt\sum_{b=0}^{h}(b+1)(-b+h+1)T(b+1)T(-b+h+1)\Big]+\\
&Rd\Big[(\theta_w-1)^3\sum_{b=0}^{h}\sum_{r=0}^{h-b}\sum_{s=0}^{h-b-r} T(b)T(r)T(s)(-b-r-s+h+2)\times\\
&\quad(-b-r-s+h+1)T(-b-r-s+h+2)\Big]+\\
&Rd\Big[3(\theta_w-1)^3\sum_{b=0}^{h}\sum_{r=0}^{h-b} T(r)T(-r+b)(-b+h+1)T(-b+h+1)(r+1)T(r+1)\Big]+\\
&Rd\Big[3(\theta_w-1)\sum_{b=0}^{h} T(-b+h)(b+1)(b+2)T(b+2)\Big]+\\
&Rd\Big[3(\theta_w-1)^2\sum_{b=0}^{h}\sum_{r=0}^{h-b} T(b)T(r)(-b-r+h+2)(-b-r+h+1)T(-b-r+h+2)\Big]+\\
&Rd\Big[6(\theta_w-1)^2\sum_{b=0}^{h}\sum_{r=0}^{h-b} T(b)(r+1)T(r+1)(-b-r+h+1)T(-b-r+h+1)\Big]+\\
&Rd\Big[3(\theta_w-1)\sum_{b=0}^{h}(b+1)(-b+h+1)T(b+1)T(-b+h+1)\Big] = 0,
\end{aligned} \tag{4.5}$$

$$(h+1)(h+2)P(h+2)+Le\sum_{b=0}^{h}(b+1)P(b+1)F(-b+h)+$$
$$\frac{Nt}{Nb}(h+1)(h+2)T(h+2)=0, \tag{4.6}$$

$$\begin{aligned}N_S =& Re\sum_{b=0}^{h}(b+1)(-b+h+1)T(b+1)T(-b+h+1)+\\
& ReRd\sum_{b=0}^{h}(b+1)(-b+h+1)T(b+1)T(-b+h+1)+\\
& ReRd(\theta_w-1)^3\sum_{b=0}^{h}\sum_{r=0}^{h-b}\sum_{s=0}^{h-b-r}\sum_{t=0}^{h-b-r-s}(b+1)T(b+1)(r+1)T(r+1)\times\\
& T(s)T(-b-r-s+h-t)T(t)+\\
& 3ReRd(\theta_w-1)\sum_{b=0}^{h}\sum_{r=0}^{h-b}T(b)(r+1)T(r+1)(-b-r+h+1)T(-b-r+h+1)+\\
& 3ReRd(\theta_w-1)^2\sum_{b=0}^{h}\sum_{r=0}^{h-b}T(r)T(-r+b)(-b+h+1)T(-b+h+1)(r+1)T(r+1)+\\
& Re\,\varepsilon(\frac{\Omega}{\varepsilon})^2\sum_{b=0}^{h}(b+1)(-b+h+1)P(b+1)P(-b+h+1)+\\
& Re\,\varepsilon(\frac{\Omega}{\varepsilon})\sum_{b=0}^{h}(b+1)(-b+h+1)T(b+1)P(-b+h+1).\end{aligned} \tag{4.7}$$

Transformed boundary conditions are

$$\begin{aligned}&F(0)=S,\ F(1)=1+\delta\ F(2),\ F(2)=\frac{n_1}{2},\ F(3)=\frac{n_2}{6},\\
&T(0)=1,\ P(0)=1,\ T(1)=n_3,\ P(1)=n_4.\end{aligned} \tag{4.8}$$

Differential transform of $f(\eta)$, $\theta(\eta)$, $\phi(\eta)$ are $F(k)$, $T(k)$, $P(k)$ and with the help of boundary conditions (2.14) and (2.15), we can find constants n_1, n_2, n_3 and n_4.

By using Eq. (4.8) we get the following iterations,

$$F[4]=\frac{1}{24\ S\beta}[n_2+S\beta\ n_1+(1+\lambda)S\ n_1-(1+\lambda)(1+\lambda\ n_1)^2],$$

$$T[2]=-\frac{Pr(S\ n_3+Nb\ n_3\ n_4+Nt\ n_3^2)-3\ Rd\ (\theta_w-1)n_3^2\ (1+(\theta_w-1))^2}{2(1+Rd)+2Rd\ (\theta_w-1)^3+6Rd\ (\theta_w-1)+6Rd\ (\theta_w-1)^2},$$

$$P[2]=-\frac{1}{2}[-2\frac{Nt}{Nb}\frac{Pr(S\ n_3+Nb\ n_3\ n_4+Nt\ n_3^2)-3\ Rd\ (\theta_w-1)n_3^2\ (1+(\theta_w-1))^2}{2(1+Rd)+2Rd\ (\theta_w-1)^3+6Rd\ (\theta_w-1)+6Rd\ (\theta_w-1)^2}+Le\ S\ n_4].$$

Putting these iterations in Eq. (4.3), we obtain the following closed form of solutions,

$$f(\eta)=S+(1+\delta\ \frac{n_1}{2})\eta+\frac{n_2}{2}\ \eta^2+\cdots$$

$$\theta(\eta) = 1 + n_3\,\eta - \frac{Pr(S\,n_3 + Nb\,n_3\,n_4 + Nt\,n_3^2) - 3\,Rd\,(\theta_w - 1)n_3^2\,(1 + (\theta_w - 1))^2}{2(1 + Rd) + 2Rd\,(\theta_w - 1)^3 + 6Rd\,(\theta_w - 1) + 6Rd\,(\theta_w - 1)^2}\,\eta^2 + \cdots$$

$$\phi(\eta) = 1 + n_4\,\eta - \frac{1}{2}[\frac{-2Nt}{Nb}\frac{Pr(S\,n_3 + Nb\,n_3\,n_4 + Nt\,n_3^2) - 3\,Rd\,(\theta_w - 1)n_3^2\,(1 + (\theta_w - 1))^2}{2(1 + Rd) + 2Rd\,(\theta_w - 1)^3 + 6Rd\,(\theta_w - 1) + 6Rd\,(\theta_w - 1)^2} + Le\,S\,n_4]\,\eta^2 + \cdots$$

5. Result and discussion

To illustrate the characteristics of the problem, the results are exhibited in Figures 2–13 and are discussed in detail. The accuracy of impact of slip parameter on coefficient of skin friction by using DTM and numerical method is illustrated in Table 1 and good agreement is found. Also the matching between these two methods can be seen in Figure 14.

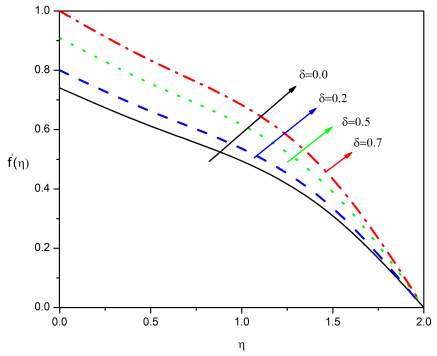

Figure 2 Variation of $f'(\eta)$ on δ when $\beta = 1$, $S = 2$, $\delta = 0$

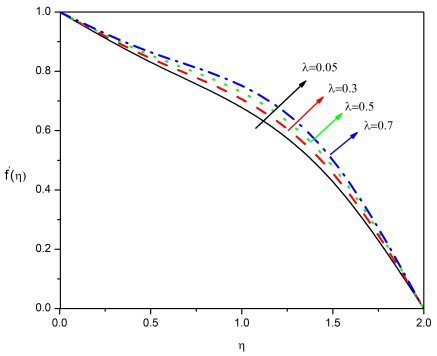

Figure 3 Variation of $f'(\eta)$ on λ when $\beta = 1$, $S = 2$, $\delta = 0$

Figure 2 shows that velocity profile increases as value of slip parameter δ increases. Slip at the surface wall rises and as a result slip at the surface wall reaches to a lesser amount of penetration due to the stretching surface into the fluid. Figure 3 shows that velocity profile increases as ratio of relaxation to retardation times parameter λ increases. Physically, as λ increases, retardation

time begins to degrade. Particles go rapidly as time consumption of particles to move from disturbed to balanced system degrades. Hence, velocity rises. Figure 4 shows that velocity profile reduces as Deborah number β rises. Because, λ_1 is dependent on retardation time and λ_1 is an increasing function of β. Hence, velocity degrades whenever particles consume much time.

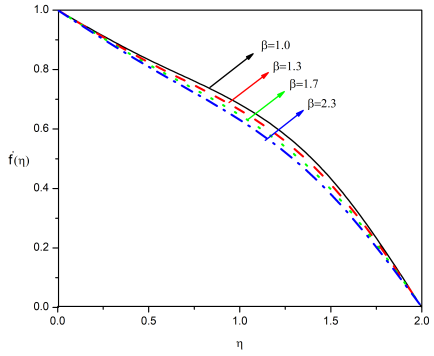

Figure 4 Variation of $f'(\eta)$ on β when $\lambda = 0.1$, $S = 2$, $\delta = 0$

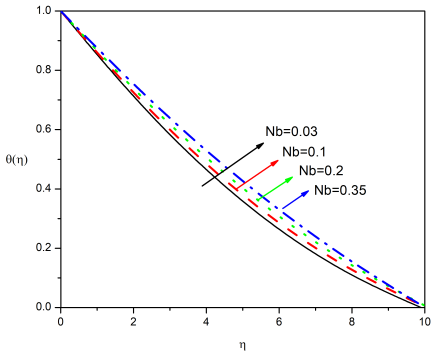

Figure 5 Variation of $\theta(\eta)$ on Nb when $S = 0.1$, $Pr = 1$, $Le = 1$, $\theta_w = 1.1$, $Rd = 0.1$, $Nt = 0.05$

Figures 5 and 6 illustrate the impact of Brownian motion parameter Nb and thermophoresis parameter Nt on temperature profile. As Nb and Nt rise, the arbitrary movement of the nanoparticles rises. This arbitrary movement of the nanoparticles generates more heat. Therefore, temperature profile rises. The variation of thermal radiation parameter Rd on $\theta(\eta)$ is explained in Figure 7. As, Rd delivers the heat energy into the flow, internal conductivity of the fluid directs the fluid flow to be hotter hence with the rise of Rd, $\theta(\eta)$ enhances.

Figure 8 shows that as Prandtl number Pr increases, temperature profile reduces. Larger viscous diffusivity and weaker thermal diffusivity can be seen in fluids having higher Pr. Because of this variation in fluids, thermal boundary layer thickness reduces. Hence, $\theta(\eta)$ reduces. Figure 9 shows that as Lewis number Le rises, nanoparticle volume fraction profile degrades. Le and Brownian diffusion coefficient are of opposite behaviour. As Le rises, Brownian diffusion coeffi-

cient reduces. Because of this reduction, nanoparticle volume fraction profile degrades. Figure 10 shows that as values of S rises, nanoparticle volume fraction profile reduces.

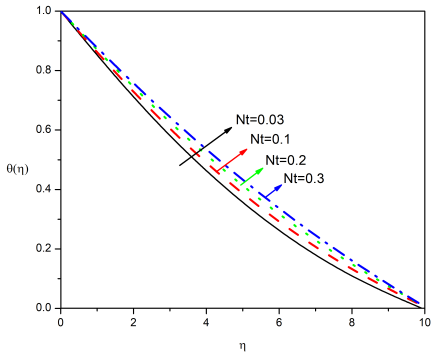

Figure 6 Variation of $\theta(\eta)$ on Nt when $S = 0.1$, $Pr = 1$, $Le = 1$, $\theta_w = 1.1$, $Rd = 0.1$, $Nb = 0.05$

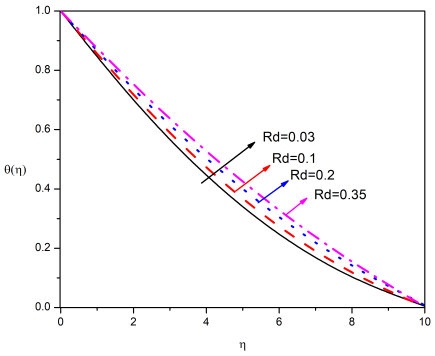

Figure 7 Variation of $\theta(\eta)$ on Rd when $S = 0.1$, $Pr = 1$, $Le = 1$, $\theta_w = 1.1$, $Nt = 0.05$, $Nb = 0.05$

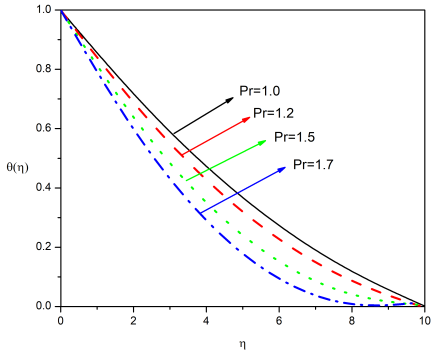

Figure 8 Variation of $\theta(\eta)$ on Pr when $S = 0.1$, $Pr = 1$, $Le = 1$, $\theta_w = 1.1$, $Rd = 0.1$, $Nb = 0.05$, $Nt = 0.05$

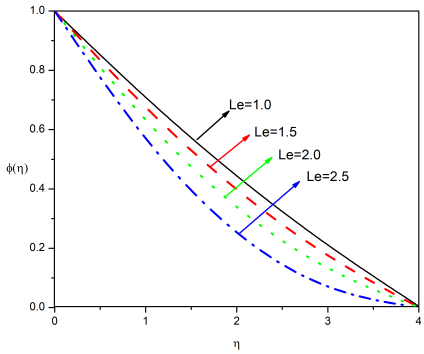

Figure 9 Variation of $\phi(\eta)$ on Le when $S = 0.1$, $Pr = 2$, $\theta_w = 1.1$, $Rd = 1$, $Nb = 0.1$, $Nt = 0.1$

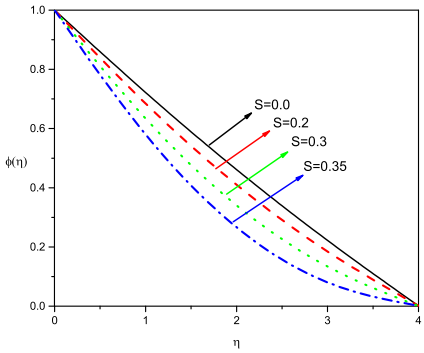

Figure 10 Variation of $\phi(\eta)$ on S when $Nt = 0.1$, $Pr = 2$, $Le = 1$, $\theta_w = 1.1$, $Rd = 1$, $Nb = 0.1$

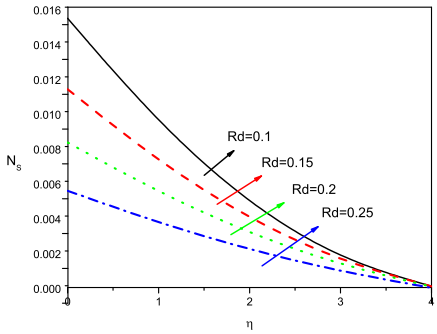

Figure 11 Variation of Rd on entropy generation when $S = 0.1$, $Pr = 2$, $Le = 1$, $\theta_w = 1.1$, $Nt = 0.1$, $Nb = 0.1$, $\varepsilon = 0.0001$, $\Omega = 1$, $\sum = 1$, $Re = 0.1$, $\delta = 0$

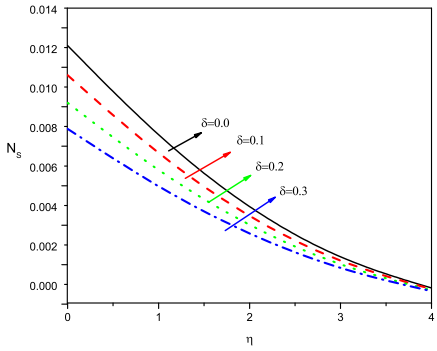

Figure 12 Variation of δ on entropy generation when $S = 0.1$, $Pr = 2$, $Le = 1$, $\theta_w = 1.1$, $Rd = 0.1$, $\sum = 1$, $\Omega = 1$, $Re = 0.1$, $\varepsilon = 0.0001$, $Nb = 0.1$, $Nt = 0.1$

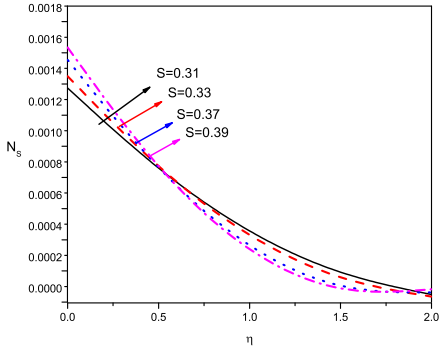

Figure 13 Variation of S on entropy generation when $Re = 0.1$, $Pr = 2$, $Le = 1$, $\theta_w = 1.1$, $Rd = 0.1$, $Nb = 0.1$, $\sum = 1$, $\Omega = 1$, $\varepsilon = 0.0001$, $\delta = 0$, $Nt = 0.1$

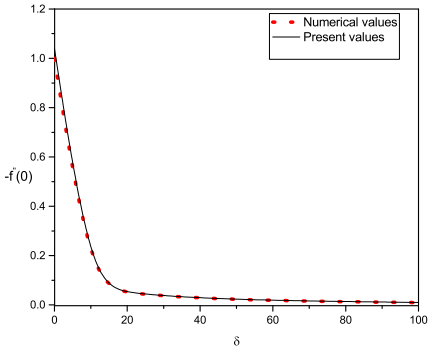

Figure 14 Comparision graph of skin friction coefficient on δ

On entropy generation the impact of Rd is given in Figure 11. Entropy generation profile reduces as value of Rd rises. This is because, the transfer of heat energy is observed in the

entropy production. Effect of δ on entropy generation is shown in Figure 12. In the vicinity of the sheet, reduction in entropy generation number is observed as δ rises. However, partial slip effect can be neglected when the distance becomes larger. In Figure 13, the effect of S on entropy generation is given. It is noted that, as the value of S rises, the entropy generation rises. Near the surface, the entropy generation rate rises as the value of S rises.

Coefficient of skin friction on various values of δ is compared with the previous studies by Bhattacharyya et al. [16] using numerical method (Shooting technique with fourth-order Runge-Kutta) and present studies. It is clear that present and previous studies are in good agreement.

δ	Bhattacharyya et al. [16]	Present study
0	-1.0000	-1.00004
0.1	-0.88602	-0.88601
0.2	-0.78764	-0.78761
1	-0.43002	-0.43021
2	-0.28890	-0.28898
10	-0.08299	-0.08299
20	-0.04480	-0.04479
50	-0.01899	-0.01899
100	-0.00953	-0.00953

Table 1 Coefficient of skin-friction $f''(0)$ for δ with $\lambda = 0$, $S = 0$, $\beta = 0$

6. Conclusions

Effects of entropy generation and nonlinear thermal radiation on Jeffery nanofluid over permeable stretching sheet with partial slip have been studied. The accuracy of impact of slip parameter on coefficient of skin friction by using DTM and numerical method (Shooting technique with fourth-order Runge–Kutta) is illustrated in Table 1 and good agreement is found. Further, the novelty and the accuracy of these two methods can be seen in Figure 14. The outcome of various parameters is given below:

▶ For larger value of S, the nanoparticle volume fraction profile decreases whereas entropy generation profile increases.

▶ As value of δ rises, the velocity profile increases and entropy generation profile reduces.

▶ By increasing the values of Rd, the temperature profile enhances whereas entropy generation profile reduces.

▶ As Le rises, the nanoparticle volume fraction profile reduces.

▶ As Nb and Nt rise, the temperature profile rises.

▶ Comparison of skin friction coefficient for δ is in good agreement with the present as well as previous studies.

Disclosure statement We report that we have no potential conflict of interest with any other author.

References

[1] L. J. CRANE. *Flow past a stretching plate*. Z. Angew. Math. Phys., 1970, **21**(4): 645–647.

[2] A. ISHAK, R. NAZAR, I. POP. *Heat transfer over a stretching surface with variable heat flux in micropolar fluids*. Phys. Letts. A, 2008, **372**(5): 559–561.

[3] V. M. SOUNDALGEKAR, T. V. RAMANA MURTHY. *Heat transfer past a continuous moving plate with variable temperature*. Warme Stoffubertrag, 1980, **14**(2): 91–93.

[4] L. G. GRUBKA, K. M. BOBBA. *Heat transfer characteristics of a continuous stretching surface with variable temperature*. ASME J. Heat Transfer, 1985, **107**(1): 248–250.

[5] A. ISHAK, R. NAZAR, I. POP. *Boundary layer flow and heat transfer over an unsteady stretching vertical surface*. Meccanica, 2009, **44**(4): 369–375.

[6] M. QASIM, T. HAYAT, S. OBAIDAT. *Radiation effect on the mixed convection flow of a viscoelastic fluid along an inclined stretching sheet*. Z. Naturforsch. A, 2012, **67**: 195–202.

[7] C. L. M. H. NAVIER. *Memoire Sur Les Lois Du Mouvement Des Fluides*. Mem. Acad. Roy. Sci. Inst., France, 1823, **6**: 389–440.

[8] Y. D. SHIKHMURZAEV. *The moving contact line on a smooth solid surface*. Int. J. Multiph. Flow, 1993, **19**(4): 589–610.

[9] C. H. CHOI, K. J. A. WESTIN, K. S. BREUER. *To slip or not to slip: Water flows in hydrophilic and hydrophobic microchannels*. International Mechanical Engineering Conference and Exposition, New Orleans, Louisiana, 2002, 557–564.

[10] M. T. MATTHEWS, J. M. HILL. *Nano boundary layer equation with nonlinear Navier boundary condition*. J. Math. Anal. Appl., 2007, **333**(1): 381–400.

[11] S. DAS, R. N. JANA, O. D. MAKINDE. *MHD boundary layer slip flow and heat transfer of nanofluid past a vertical stretching sheet with non-Uniform heat generation/absorption*. Int. J. Nanosci., 2014, **13**(3): 1450019, 12 pp.

[12] R. DODDA, R. SRINIVASA RAJU, J. A. RAO, et al. *Boundary layer viscous flow of nanofluids and heat transfer over a nonlinearly isothermal stretching sheet in the presence of heat generation/absorption and slip boundary conditions*. Int. J. Nanosci. Nanotechnol., 2016, **12**(4): 251–268.

[13] P. D. ARIEL, T. HAYAT, S. ASGHAR. *The flow of an elastico-viscous fluid past a stretching sheet with partial slip*. Acta Mech., 2006, **187**(1): 29–35.

[14] Z. ABBAS, Y. WANG, T. HAYAT, et al. *Slip effects and heat transfer analysis in a viscous fluid over an oscillatory stretching surface*. Int. J. Numer. Meth. Fluids, 2009, **59**(4): 443–458.

[15] C. Y. WANG. *Flow due to a stretching boundary with partial slip an exact solution of the Navier-Stokes equations*. Chem. Eng. Sci., 2002, **57**(17): 3745–3747.

[16] K. BHATTACHARYYA, M. S. UDDIN, G. C. LAYEK. *Effect of partial slip on boundary layer mixed convective flow adjacent to a vertical permeable stretching sheet in porous medium*. Acta Tech., 2013, **58**(1): 27–39.

[17] K. DAS. *Nanaofluid flow over a non-linear permeable stretching sheet with partial slip*. J. Egypt. Math. Soc., 2015, **23**(2): 451–456.

[18] S. ITTEDI, R. DODDA, S. JOG. *Partial slip effect of MHD boundary layer flow of nanofluids and radiative heat transfer over a permeable stretching sheet*. Glob. J. Pure Appl. Math., 2017, **13**(7): 3083–3103.

[19] K. DAS. *Slip flow and convective heat transfer of nanofluids over a permeable stretching surface*. Comput. Fluids, 2012, **64**: 34–42.

[20] S. MUKHOPADHYAY, R. S. R. GORLA. *Effects of partial slip on boundary layer flow past a permeable exponential stretching sheet in presence of thermal radiation*. Heat Mass Transfer, 2012, **48**(10): 1773–1781.

[21] M. A. HOSSAIN, H. S. TAKHAR. *Radiation effect on mixed convection along a vertical plate with uniform surface temperatur*. Heat and Mass Transfer, 1996, **31**(4): 243–248.

[22] H. S. TAKHAR, R. S. R. GORLA, V. M. SOUNDALGEKAR. *Radiation effects on MHD free convection flow of a gas past a semi-infinite vertical plate*. Int. J. Nume. Meth. Heat Fluid Flow, 1996, **6**(2): 77–83.

[23] M. A. HOSSAIN, M. A. ALIM, D. A. S. REES. *The effect of radiation on free convection from a porous vertical plate*. Int. J. Heat Mass Transf., 1999, **42**(1): 181–191.

[24] A. BEJAN. *A study of entropy generation in fundamental convective heat transfer*. J. Heat Transfer, 1979, **101**(4): 718–725.

[25] A. NOGHREHABADI, M. R. SAFFARIAN, R. POURRAJAB, et al. *Entropy analysis for nanofluid flow over a stretching sheet in the presence of heat generation/absorption and partial slip*. J. Mech. Sci. Technol., 2013, **27**(3): 927–937.

[26] Muhammad Mubashir BHATTI, T. ABBAS, Mohammad Mehdi RASHIDI. *Numerical study of entropy generation with nonlinear thermal radiation on magnetohydrodynamics non-Newtonian nanofluid through a porous shrinking sheet*. J. Magn., 2016, **21**(3): 468–475.

[27] M. GOVINDARAJU, N. VISHNU GANESH, B. GANGA, et al. *Entropy generation analysis of magnetohydrodynamic flow of a nanofluid over a stretching sheet*. J. Egypt. Math. Soc., 2015, **23**: 429–434.

[28] M. ALMAKKI, H. MONDAL, P. SIBANDA. *Entropy generation in mhd flow of viscoelastic nanofluids with homogeneous-heterogeneous reaction, partial slip and nonlinear thermal radiation*. J. Therm. Eng., 2020, **6**(3): 327–345.

[29] B. GANGA, M. GOVINDARAJU, A. K. ABDUL HAKEEM. *Effects of inclined magnetic field on entropy generation in nanofluid over a stretching sheet with partial slip and nonlinear thermal radiation*. Iran J. Sci. Technol. Trans. Mech. Eng., 2019, **43**(4): 707–718.

[30] M. QASIM. *Heat and mass transfer in a Jeffrey fluid over a stretching sheet with heat source/sink*. Alex. Eng. J., 2013, **52**(4): 571–575.

[31] M. B. ASHRAF, T. HAYAT, A. ALSAEDI, et al. *Convective heat and mass transfer in MHD mixed convection flow of Jeffrey nanofluid over a radially stretching surface with thermal radiation*. J. Cent. South Univ., 2015, **22**(3): 1114–1123.

[32] T. HAYAT, G. BASHIR, A. ALSAEDI, et al. *MHD flow of Jeffery liquid due to a nonlinear radially stretched sheet in the presence of Newtonian heating*. Results Phys., 2016, **6**: 817–823.

[33] T. HAYAT, S. ASAD, M. QASIM, et al. *Boundary layer flow of a Jeffrey fluid with convective boundary conditions*. Int. J. Numer. Meth. Fluids, 2012, **69**(8): 1350–1362.

[34] T. HAYAT, Z. IQBAL, M. MUSTAFA, et al. *Unsteady flow and heat transfer of Jeffrey fluid over a stretching sheet*. Therm. Sci., 2014, **18**(4): 1069–1078.

[35] K. DAS, N. ACHARYA, P. K. KUNDU. *Radiative flow of MHD Jeffrey fluid past a stretching sheet with surface slip and melting heat transfer*. Alex. Eng. J., 2015, **54**: 815–821.

[36] Hu Ge-JiLe, S. QAYYUM, F. SHAH, et al. *Slip flow of Jeffrey nanofluid with activation energy and entropy generation applications*. Adv. Mech. Eng., 2021, **13**(3): 1–9.

[37] S. SEPASGOZAR, M. FARAJI, P. VALIPOUR. *Application of differential transformation method (DTM) for heat and mass transfer in a porous channel*. Propuls. Power Res., 2017, **6**(1): 41–48.

[38] A. MIRZAAGHAIAN, D. D. GANJI. *Application of differential transformation method in micropolar fluid flow and heat transfer through permeable walls*. Alex. Eng. J., 2016, **55**(3): 2183–2191.

[39] M. HATAMI, Dengwei JING. *Differential transformation method for Newtonian and non-Newtonian nanofluids flow analysis: compared to numerical solution*. Alex. Eng. J., 2016, **55**: 731–739.

[40] M. M. A. KHATER. *Abundant breather and semi-analytical investigation: On high-frequency waves's dynamics in the relaxation medium*. Modern Phys. Lett. B, 2021, **35**(22): Paper No. 2150372, 17 pp.

[41] M. M. A. KHATER, S. K. ELAGAN, M. A. El-SHORBAGY, et al. *Folded novel accurate analytical and semi-analytical solutions of a generalized Calogero-Bogoyavlenskii-Schiff equation*. Commun. Theor. Phys. (Beijing), 2021, **73**(9): Paper No. 095003, 11 pp.

[42] M. M. A. KHATER, Dianchen LU. *Analytical versus numerical solutions of the nonlinear fractional time-space telegraph equation*. Modern Phys. Lett. B, 2021, **35**(19): Paper No. 2150324, 13 pp.

[43] M. M. A. KHATER, T. A. NOFAL, H. ABU-ZINADAH, et al. *Novel computational and accurate numerical solutions of the modified Benjamin-Bona-Mahony (BBM) equation arising in the optical illusions field*. Alex. Eng. J., 2021, **60**(1): 1797–1806.

[44] M. M. A. KHATER, A. A. MOUSA, M. A. EL-SHORBAGY, et al. *Analytical and semi-analytical solutions for Phi-four equation through three recent schemes*. Results Phys., 2021, **22**: 103954.

[45] Yuming CHU, M. M. A. KHATER, Y. S. HAMED. *Diverse novel analytical and semi-analytical solutions of the generalized* $(2+1)$*-dimensional shallow water waves model*. AIP Advances, 2021, **11**: 015223.